1.1 The Status of the BNL R&D ERL

Ilan Ben-Zvi, Zeynep Altinbas, Dana Beavis, Sergey Belomestnykh, Jin Dai, Leonard DeSanto, David Gassner, Lee Hammons, Harald Hahn, Ady Hershcovitch, Animesh Jain, Puneet Jain, James Jamilkowski, Dmitry Kayran, Nikolaos Laloudakis, Robert Lambiase, Dewey Lederle, Eduard Lessard, Xue Liang, Vladimir Litvinenko, Chuyu Liu, George Mahler, Michael Mapes, Gary McIntyre, Robert Michnoff, Wuzheng Meng, Toby Miller, David Pate, Phillip Pile, David Phillips, Stephen Pontieri, Jonathan Reich, Thomas Roser, Miguel Ruiz Osés, Carl Schultheiss, Thomas Seda, Brian Sheehy, John Smedley, Triveni Rao, Kevin Smith, Roberto Than, Robert Todd, Joseph Tuozzolo, Erdong Wang, Daniel Weiss, Michelle Wilinski, Wencan Xu, Alexander Zaltsman.

Mail to: mailto: benzvi@bnl.gov
Collider-Accelerator Department, Brookhaven National Laboratory, USA

1.1.1 Introduction

The Collider-Accelerator Department at Brookhaven National Laboratory is building a high-brightness 500 mA capable Energy Recovery Linac (ERL) as one of its main R&D thrusts towards eRHIC, the polarized electron – hadron collider as an upgrade of the operating RHIC facility. The ERL is in final assembly stages, with injection commisioning starting in October 2012. The objective of this ERL is to serve as a platform for R&D into high current ERL, in particular issues of halo generation and control, Higher-Order Mode (HOM) issues, coherent emissions for the beam and high-brightness, high-power beam generation and preservation. The R&D ERL features a superconducting laser-photocathode RF gun with a high quantum efficiency photoccathode served with a load-lock cathode delivery system, a highly damped 5-cell accelerating cavity, a highly flexible single-pass loop and a comprehensive system of beam instrumentation. In this ICFA Beam Dynamics Newsletter article we will describe the ERL in a degree of detail that is not usually found in regular publications. We will discuss the various systems of the ERL, following the electrons from the photocathode to the beam dump, cover the control system, machine protection etc and summarize with the status of the ERL systems.

1.1.2 Elements of the BNL ERL

1.1.2.1 *Photocathode*

It is natural to start the description of the ERL from the photocathode, where the electron beam is born, and where its initial emittance is constrained.

The design of photocathodes for ERLs is one of the key challenges for these machines. In particular, various applications, like X-ray sources and hadron cooling require very low transverse emittance electron beams from the cathode as well as high Quantum Efficiency (QE) at visible wavelengths. This latter requirement is driven by the need to have efficient transverse and longitudinal pulse shaping and by the desirability of using compact and efficient laser sources, such as fiber lasers as the

excitation source. To meet these requirements, we have been working on green sensitive, low emittance and highly efficient photocathodes based on K_2CsSb in collaboration with Stony Brook University and Lawrence Berkeley Laboratory. Some of the results were reported [1] on their fabrication, QE, transverse emittance and robustness under laser illumination and exposure to contamination that might be expected in a photo-gun. To briefly summarize our results, the maximum QE reached was typically 6% at 532 nm. We find a 50% decay time for QE at 532 nm to be around 17 hours for water partial pressure of $2x10^{-9}$ mBar. As the partial pressure of water in the superconducting RF gun is vanishingly small, the cathode lifetime given by residual vacuum is quite acceptable. In addition, when illuminated with a laser focused to a spot diameter of 100 μm, a current density of 100 mA/cm^2 could be maintained without deterioration over the course of a measurement lasting several days. Finally, we measured a thermal emittance of 0.37 microns / mm-rms at 532 nm laser wavelength.

In addition to the multi alkali photocathode, the collaboration also carries out R&D on Diamond Amplified Photocathodes (DAP) but we will not elaborate here on this subject but provide references for the interested reader [2].

Insertion of photocathodes in the ERL superconducting RF electron gun presents special challenges. The cathode system includes a preparation chamber and two cathode transporters making up a “load-lock” system.

The purpose of the photocathode deposition and transport system is to produce a robust, high yield multialkali photocathode away from the injector complex and have a method of transporting the multialkali photocathode for insertion into a super conducting RF electron gun. This process is only successful if the high quantum efficiency is maintained during the transport and insertion in the SRF electron gun,. One important element in producing and maintaining a high QE multialkali photocathode maintaining the strict vacuum requirements of 10^{-11} torr. We have developed numerous multi-alkali deposition systems for a number of years. Our third generation system is a load-lock system, comprising a preparation chamber and transport carts, designed and produced by Advanced Energy Systems Inc. of Medford NY (AES), modified and adapted by BNL.

There are certain design criteria and principles required. One must be able to install, remove, rejuvenate and replace a cathode without exposing the source or cathode to atmosphere. The system must allow one to deposit Cs, K, and Sb on a cathode tip surface at pressures in the 10^{-10} torr range. The cathode needs to be heated to as high as 850 degrees C for cleaning and maintained at 130 degrees C to 150 degrees C during deposition. There should also be the capability for in-situ quantum efficiency (QE) measurements. Finally the transport cart must be mobile and be able to negotiate the ERL facility labyrinth, couple to the SRF gun and insert the cathode into the gun.

1.1.2.2 *Laser system*

The laser systems of the ERL comprise of two lasers, one for a high bunch-charge, low repetition rate of 9.38 MHz and the other for low bunch charge of 0.7 nC but a high rate of 703.5 MHz, designed to reach 500 mA in the ERL. The high repetition rate optical fiber 35-watt laser designed and built by Aculight needs some repair and is not yet commissioned, so the following detailed description is for the first laser.

Operation of the photocathode gun in the ERL requires that a tightly controlled optical pulse train, consisting of temporally and spatially shaped pulses, be delivered at

the photocathode in synchrony with the RF field in the gun cavity. The pulse train must also be dynamically variable, in order to tune or ramp up the current in the ERL. A laser was developed especially for this task by Lumera Laser GmbH, of Kaiserslautern Germany, under design supervision and review of the ERL project. Following the final design review, the laser was delivered in August 2009. Tests certifying its compliance with design specifications have been performed. The development of the necessary spatial and temporal shaping techniques is an ongoing project: proof-of-principle experiments have been successfully carried out with a laser of similar pulse width, operating at 532 nm and 81.5 MHz. A transport line has been designed and built and the propagation of a shaped pulse through it to the photocathode simulated and tested experimentally [4]. As the performance of the complete photocathode drive system is critical for ERL operation, an extensive set of diagnostics will be in place to monitor and maintain its performance. The repetition rate of 9.38 MHz is the 75th subharmonic of the RF frequency of the gun and accelerating cavity, 703.5 MHz. Synchronization with the RF field in the gun is extremely important; asynchrony impacts beam energy fluctuations, emittance, energy recovery, and ultimately overall stability. The total jitter must be less than 1 psec rms. Timing requirements also include the ability to ramp up the repetition rate of the laser while maintaining synchronization, in order to run the ERL at low repetition rate while tuning up, and ramp up its current in operation.

The optimal width of the optical pulse at the photocathode is much longer than the 10-12 picoseconds specified for the laser. The pulse shape of the drive pulse is optimally flat-topped, and the specified width for the nominally sech^2-shaped pulse from the laser was chosen to obtain, within the constraints imposed by this type of mode-locked laser, an adequately short rise and fall time in the photocathode drive pulse produced by the shaping methods described below. Similarly, the mode quality specification is driven by the mode requirements of the spatial shaping techniques. The total power requirement of 10 W at 532 nm fits a maximum ERL current of 50 mA. This current would require ~6 W of 532 nm light delivered at the photocathode, at the conservative quantum efficiency of 2%, leaving over a four-watt margin to cover losses in shaping, transport, and diagnostics, and to compensate for less than optimal quantum efficiency.

The Seeder is a mode-locked Nd:YVO4 oscillator, end-pumped with 25 W of 808 nm light, which is fiber-coupled in from diodes located in an off-board power supply. A semiconductor saturable absorber mirror (SESAM) is used for mode-locking. A White-cell multipass configuration is used to achieve the long path length required for the low, 9.38 MHz repetition rate. This is a cavity folding technique which uses a cell comprised of three mirrors of identical curvature that repeatedly image the spot to the mirror surface, each time with a small displacement, so that the beam ultimately exits the cell after a large number of traversals.

An isolation stage and a Nd:YVO4 power amplifier follow the oscillator. The 100 watts of pump light is brought in by fiber. The 2.2W, 1064 nm output of the oscillator is amplified to 20 W in the amplifier. A pulse picker follows, enabling us to select single pulses or groups of pulses at burst rates up to 1 kHz, with up to 90% duty cycle. Continuous operation at the full 9.38 MHz is also possible. The selected optical pulses are then passed sequentially through the second harmonic generation (SHG) The conversion efficiency is ~50% for the SHG.

The laser output will be shaped transversally by a π−shaper and longitudinally by pulse stacking. Space is too constrained to allow more detail here. We have simulated and tested both methods on another laser and plan to implement it in the ERL laser.

1.1.2.3 *SRF electron gun*

1.1.2.3.1 Introduction to the SRF gun

The SRF gun is a half-cell cavity that is designed to deliver 0.5A at 2MeV with 1MW of CW RF power. It incorporates a double quarter-wave (QW) choke joint cathode insert a pair of opposing fundamental power couplers (FPC), a high-temperature superconducting (HTSC) emittance compensation solenoid and damper of Higher Order Mode (HOM) [5].

The design of the gun must balance good beam dynamics for high charge bunches with damping of HOMs and a good geometry for the peak surface fields.

Among the challenges for this device are achieving the high RF coupling (external Q of 37,000) without excessive FPC probe penetration, while engineering a compact cavity configuration that addresses the high-power thermal issues. The coupler port and entire liquid helium vessel underwent significant adjustment to increase the coupling. Another challenge, possibly the largest, is the introduction of a removable cathode and choke joint that yields adequate cathode lifetime, avoids cavity contamination when using the base-line multi-alkali cathodes and avoid multipacting that cannot be conditioned. Yet another challenge - an emittance compensation solenoid has to be inserted close to the gun in the cryostat, but one that keeps the field on the superconductor low enough. Finally, the HOM power has to be drained from the gun cavity to avoid cryogenic losses or emittance dilution.

1.1.2.3.2 The cavity design

The cavity iris had to be made small for beam dynamics reasons (reduction of effective length of the cavity). That precluded damping all HOMs through the beam pipe.

At a beam pipe diameter of 10 cm, the same as the iris of the cavity, most of the HOMs propagate adequately to the load. The reduced beam pipe size simplifies the strong coupling of the 1 MW RF power to the beam and reduces the size of the exit vacuum valve.

The cavity was fabricated utilizing both RRR-300 Nb sheet and ingot material. This was necessary as the back surface of the cavity and the base of the choke joint region needed to be machined from one piece to ease the welding and fabrication processes, as well as to produce a cavity that could be built and inspected as required by the ASME code. The helium vessel for the cavity is titanium, which is then surrounded by multi-layer super-insulation and then two layers of mu-metal magnetic shielding with a liquid nitrogen shield in between them and then the space frame, which supports all of the aforementioned structures. The ballast tank will then be installed over the cavity, insulated and then lowered into the rectangular vacuum vessel.

1.1.2.3.3 The cathode insertion system

The cathodes are deposited on the tip of an insert. The insert can be moved from the cathode preparation system to the gun. The insert has a triple choke-joint design to allow thermal isolation of the cathode insert from the gun body while sealing the RF

currents. The choke joint innermost conductors are grooved. This grooved design reduces significantly the strength of multipacting in the choke joint. The cathode insert is introduced into the gun beam-line vacuum through a pair of gate-valves, one on the transport cart and one on the gun cathode-side line. Once the insert is near its correct position, a special fork is motor-driven to grab the insert and press it to a pre-determined load to its exact final position, making the RF seal between the insert's choke joint and the gun body. The fork motor and gear is located in the insulating vacuum, to avoid the introduction of particulate matter into the gun.

1.1.2.3.4 The Fundamental Power Couplers

One of the key features that required extensive analysis was the FPC and the shape of the tip of the antenna. After several iterations it was decided to use an antenna tip that matched the radius of the beampipe of the injector. This "pringle" tip is shown in figure 2, and provides a very nice way to achieve the desired Q external of the FPC (3e4) while not penetrating the beampipe as one would have to do with a standard antenna.

The FPCs were conditioned before installation in the gun on a special stand, which allowed us to expose them to 125 kW CW and 250 kW pulsed power in standing wave with a variable reflection phase. Various multipacting regions were encountered and processed completely [6].

1.1.2.3.5 High temperature superconducting emittance compensation solenoid

The final key item is the high temperature superconducting solenoid that is being placed at the end of the cavity to help focus the electron beam on it's way to the accelerating cavity. This solenoid has been designed and built by Ramesh Gupta and the Superconducting Magnet Division at BNL and has already undergone its acceptance testing. The solenoid is design to provide a field of 0.014 Tesla (integral of field squared 0.001 meter Tesla squared) while keeping the stray fields that reach the cavity to below 10 mGauss. This has been accomplished by using a bucking coil adjacent to the primary coil, and by moving the magnetic shielding in between the solenoid and the cavity. The coils are made with a tape of the HTS material Bi2223 with spiral wrapped Kapton insulation. A detailed description of both the solenoid design and the simulation data can be found in the reference [7]

1.1.2.3.6 The Higher Order Mode damping

The gun propagates all but 3 of the HOMs down the beam pipe to a room temperature ferrite HOM absorber. The 3 trapped modes can be easily missed by harmonics of the beam repetition frequency and detailed calculations have shown that the effect of long range wake fields can be neglected if the beam amplitude and phase noise are under a reasonable limit. It is expected that the strong coupling of the fundamental power couplers will damp some or all of these modes. Work is in progress on this question.

The HOM analysis for this cavity was carried out using ABCI and later microwave studio. The total HOM power dissipated by a 500 mA, 1.4 nC beam was calculated to be ~0.5 kW. [5] Due to the frequency of the injector the harmonics spectrum is fairly sparse and spread out and avoids overlapping with any HOMs.

1.1.2.4 *SRF Accelerating Cavity*

The BNL 5-cell ampere-class cavity was constructed in collaboration with AES and BCP processed at JLab. The BNL design aims to address the most extreme HOM conditions by virtue of its low frequency (703.75 MHz), small number of cells (5) and very good damping of HOMs.

1.1.2.4.1 HOM Damping

The loss factor of SRF cavities varies considerably from under 1 V/pC up to 10 V/pC, depending on the structure's frequency (the lower the frequency the better), the degree to which the cavity aperture has been maximized (possibly sacrificing some other parameter) and the number of cells (the fewer the better). Beam properties enter in three places: The HOM power is proportional to the average current to the bunch charge, and (through the loss factor, approximately) to the square root of the pulse length. Good damping of the HOM power is important for a number of reasons. First, one has to remove this power from being intercepted at cryogenic temperatures, increase the threshold for beam-breakup (BBU) and to avoid beam quality degradation.
The cavity has very large cavity irises (17 cm diameter) and extremely large beam pipe, 24 cm in diameter. The beam pipe is large enough to propagate all the HOMs to the ferrite HOM loads, which are at room temperature on either side of the cavity. The HOM dampers are commercially available, derived from the Cornell 500 MHz storage ring cavity design. As a result of these design features the cavity is a "single mode" cavity, all HOMs are strongly coupled to the HOM damper, and the loss factor is very low [8]. The cell shape also enhances mechanical stability.

1.1.2.5 *Radio Frequency Power*

The Energy Recovery Linac requires two high power RF systems. The first RF system is for the 703.75 MHz superconducting electron gun. The RF power from this system is used to drive nearly half an Ampere of beam current to 2.5 MeV. There is no provision to recover any of this energy so the minimum amplifier power is 1 MW. It consists of 1 MW CW klystron, transmitter and power supplies, 1 MW circulator, 1 MW dummy load and a two-way power splitter. The second RF system is for the 703.75 MHz superconducting cavity. The system accelerates the beam to 20 MeV and recovers this energy. It will provide up to 50 kW of CW RF power to the cavity. It consists of 50 kW transmitter, circulator, and dummy load.

1.1.2.5.1 High Power RF

1.1.2.5.1.1 The 1 MW System

There are several main equipment groups in this system. The Klystron_tube, manufactured by CPI, is rated to produce 1.0 MW CW at 703.75 MHz. This tube is similar to one produced by CPI for LANL, but the BNL tube does not have a modulating anode. The output of the tube is WR1500.

Electrical Characteristics – The collector is grounded, and -92kV at -17.1A will produce 1 MW in our tube. While the maximum drive specified for 1MW is 100W (40dB gain), this tube only requires 15.2W to get full power. The driver amplifier provided has 200 W max output, 52 dB gain.

Other tube electrical requirements include the cathode heater, two solenoid circuits, and two 8 l/s vac-ion pumps. These are all controlled and monitored by the transmitter. Cooling – There are three water cooling loops, the collector requires 380 gpm, and is not temperature controlled. The two body loops are each about 7gpm, and are temperature controlled. There are two inlets for forced air-cooling of the output window, fed from one 100 CFM blower in the transmitter. The exhaust heat in this air plus the heat put into the air by the air-cooled solenoids and other heat sources, must be removed from the radiation enclosure.

The "transmitter" manufactured by Continental Electronics Corporation is the power supply. Its basic design is to stack 96 isolated IGBT gated power supplies in series. Because the IGBTs permit a fast shut down mode, a crow bar is not required to limit the energy in an arc to 40 Joules. The transmitter also contains the support equipment for the klystron, including the filament power supply, two solenoid power supplies, two vac-ion pump controllers, several cooling water monitoring circuits, two air blowers – one for the klystron window and one for a window in the ring, a RF amplifier, and a PLC to keep track of everything, including interlocks and monitoring of directional couplers in the system.

Electrical characteristics are AC Input: 4160 VAC (chosen to match the previous design), DC Output: - 100 kV at – 21 A, filaments: 30 Vrms at 30 Arms, isolated to operate at – 100 kV, solenoid PS: 30 A at 30 V and 30 A at 300 V.

Water circuits include three at 400 gpm max (collector, RF load, beam dump), and four at 35 gpm max (body, output cavity, circulator, spare).

The unit is very efficient, as the IGBTs are switched at maximum rate of about 400 Hz. This low frequency is consistent with a high ripple frequency as timing techniques result in a fundamental ripple frequency of almost 40 kHz. The unit is entirely air-cooled.

The klystron is protected by a circulator with a water-cooled termination. This water cooled dummy load, manufactured by CML Corp, is rated for 1.3 MW of continuous power. It has a WR1500 waveguide input, a ceramic window, and a stand with six point leveling.

The water-cooled circulator is manufactured by AFT Microwave. It is rated at 1 MW into any port. The center frequency is 703.75 MHz, bandwidth: ±17 MHz. Over this bandwidth the insertion loss is < 0.1 dB, isolation > 20 dB and VSWR: < 1.2 .

1.1.2.5.1.2 The 50 kW System

The Thomson ***SIIA*** Scientific and Industrial IOT Amplifier family is adapted from the highly successful, field-proven IOX and DCX family of high power IOT UHF television broadcast transmitter line. This line of equipment has been a world standard in the television broadcast industry. Inductive Output Tube (IOT) utilized in the amplifier is the industry standard for its high efficiency (over 50%). It also provides a gain of 22 to 23 dB with remarkably low phase shift at wide range of output power.

To isolate and protect transmitter from very high VSWR we have installed a 50 kW circulator. Manufactured by AFT Corporation it performed very well.

1.1.2.5.2 Low Level RF

The low level RF system for the R&D ERL (5-cell cavity, RF gun) is a variant of a newly designed digital LLRF controller platform, recently commissioned at RHIC and

the Electron Beam Ion Source (EBIS). The central component of the LLRF hardware is a chassis referred to as a “controller”. Essentially a controller is a powerful, flexible, software/firmware configurable digital signal-processing platform, adaptable to many tasks. A controller consists of a “carrier” board together with up to six associated “daughter” mezzanine modules, which attach to the carrier via an IEEE standard XMC interface. The carrier serves as a stand-alone network attached control system interface, host platform for the daughter mezzanine modules, communication hub and diagnostic data acquisition engine. Daughter modules provide system specific functionality and signal processing horsepower – an example being a 4CH ADC board used to digitize RF signals from a cavity. All boards are custom designed at BNL, based on a common powerful Field Programmable Gate Array (FPGA) family, the Xilinx Virtex-5 FX devices. The Virtex-5 FX FPGA family provides a number of very powerful resources. Depending on the specific version used, there are either one or two hard-core PPC processors available. 16 multi-gigabit serial transceivers provide very high bandwidth communication, and even deterministic data links as needed. Hardware “DSP Slices” provide very high-speed signal processing functionality. Large arrays of programmable logic and static RAM, high speed low jitter clock generation and distribution, very large IO pin count, support for numerous single ended and differential IO standards, and relatively low power dissipation complete a feature list which we exploit to the fullest.

For the R&D ERL, two of these controllers will be integrated into a LLRF control system. To provide ultra low noise LLRF signal processing with absolute synchronism (phase lock) across multiple controllers and daughter modules, the system relies on two key components. First, an ultra low noise 100MHz master clock is distributed to both chassis, and within, to the carriers and daughter modules. This clock has a typical integrated phase noise of <100 fs rms in a 1Hz to 100kHz bandwidth (BW 1-100k). This clock is distributed within the controllers via high-speed differential PECL fan-outs, and on each daughter is used as a reference clock for a 1600MHz PLL. This PLL provides a variety of divided output clocks for on board DACs, ADCs, FPGAs, etc., with a typical integrated phase noise of about 140fs rms (BW 1-100k). The RF DACs used to provide RF drive signals produce carrier signals with phase noise of 170fs to 200fs rms (BW 1-100k), when clocked at 400 MSPS.

Second, a multi-gigabit serial link referred to as the “Update Link” and employing the same 100 MHz master clock as a reference, provides a deterministic timing in the form of an encoded “Update Pulse” event occurring every 1000 clock cycles, or at a 100kHz “Update Rate”. This Update Pulse is decoded locally at every carrier and daughter module providing deterministic timing across the system. The Update Link also broadcasts global event and data packets, which if desired can maintain a fixed timing relationship to the Update Pulse via pre-assigned “slotting” within an Update Period. An example of this would be a “Master Reset” event, used to deterministically reset all RF synthesizers to known reference phases.

The combination of these permits a complete LLRF system to be built up from the requisite number of chassis and daughter modules, while ensuring that all sub-components can maintain the desired RF phase relationships.

1.1.2.6 *Cryogenic system*

The ERL cryogenic system will supply cooling to a super-conducting RF gun and the 5-cell super-conducting RF cavity system that need to be held cold at 2K. The engineering of the cavity cryomodules were carried out by AES in collaboration with BNL. The 2K superfluid bath is produced by pumping on the bath using a sub-atmospheric warm compression system.

The cryogenic system makes use of mainly existing equipment relocated from other facilities: a 300W 4.5K coldbox, an 45 g/s screw compressor, a 3800 liter liquid helium storage dewar, a 170 m3 warm gas storage tank, and a 40,000 liter vertical low pressure liquid nitrogen storage dewar. An existing wet expander obtained from another facility has been added to increase the plant capacity. In order to deliver the required 3 to 4 bar helium to the cryomodules while using up stored liquid capacity at low pressure, a new subcooler has been installed to function as the capacity transfer device.
A 2K to 4K recovery heat exchanger is also implemented for each cryomodule to recover refrigeration below 4K, thus maximizing 2K cooling capacity with the given sub-atmospheric pump. No 4K-300K refrigeration recovery is implemented at this time of the returning sub-atmospheric cold vapor, hence the 2K load appears as a liquefaction1 load on the cryogenic plant.A separate LN2 cooling loop supplies liquid nitrogen to the superconducting gun's cathode tip. The following details the components of the system.

Sub-atmospheric pumping System: An oil injection cooled Roots blower backed by 2 liquid rings pumps is used to pump on the liquid helium bath to produce the 2K cooling. The system is capable of pumping 5.5 g/s with the bath held at 2K. The Roots blower is a Tuthill MB5400 belt geared down to 1900 rpm from the 2400 rpm max using a 40 HP motor. The blower is backed by two (2) Kinney KLRC-525 2- stage liquid ring pumps with 50 HP motors. A high to low by-pass valve controls the suction pressure at the pump from dropping below its setpoint. Coalescing element at the discharge of the each liquid ring pump prevents carry over of oil to the discharge line. The vacuum pump discharge will go to the low pressure (suction side) of the main helium plant.

4.5K Coldbox The Process Systems International 300 W @ 4.5K model 1660S built in 1993, has 2 pairs of 3 inch (76 mm) diameter piston expanders, configured as a Collins cycle with liquid nitrogen precooling. The first expansion stage operates at an inlet of 50K, and the second expansion stage at an inlet of ~19K in liquefaction mode.

Wet expander A 1985 Koch Process System wet expander consisting of a pair of 2 inch (50 mm) diameter piston has been added to the system, providing an additional 0.7 g/s liquefaction capacity to the plant.

Main compressor The main helium compressor is a 1975 Sullair C20LA4.8-400HP screw compressor, complete with bulk oil separator. The oil demisting system consists of 2 parallel banks of 4 Balston coalescing elements in series: DX, BX, BX, BX. A 18 inch diameter charcoal bed is used for oil vapor removal. Flow throughput of the compressor is 45 g/s @ 1.05 atm.

Liquid helium inventory Liquid helium inventory will be stored in an existing 3800 liters liquid helium storage dewar manufactured in 1992 by Cryofab. The dewar has 3 liquid fill and one vapor line as interface.

Gas Storage Tank An existing 170 m^3 warm gas storage tank is used for inventory storage when the system is warm.

Subcooler

Because helium at 3 to 4 bar is required for the intercept flows in the cryomodules, the plant's high pressure flow is used to supply the cryomodules, instead of low pressure liquid from the storage dewar. The subcooler serves to condition the plant's warmer liquid helium to 4.5K and simultaneously serves to use-up liquid inventory from the main low-pressure storage dewar.

5-cell valvebox

A valvebox containing the 2K-4K recovery heatexchanger, top fill valve, cooldown/fill valve, vapor return control valve and equalization valve between the cooldown line and vaporspace provides helium to the 550 liters reservoir above the cavity cryostat.

5-Cell Cryostat and Reservoir

A 550 liter reservoir, above the 5-cell cavity allows the system to operate for a while without filling with liquid helium from the cryogenic system. This will allow the subatmospheric pump to handle the maximum heat load when required. 4 intercept circuits using 3 bar liquid helium to intercept the 2 beam tube cold to warm transitions, and fundamental power coupler outer conductor, and tuner mass cooling are returned after warming to room temperature using electric heaters, to each thermal mass flow controller located outside the radiation blockhouse. The cryostat also has a liquid nitrogen cooled shield that surrounds the cavity.

SRF Gun valvebox

This valvebox contain the helium vapor return control valve, liquid nitrogen cooling loop for the cold cathode head. The liquid nitrogen cooling loop consists of a phase separator to provide liquid to the cathode head, and the returning 2 phase flow is returned, except for the flex line section, in a coaxial arrangement to intercept the heat leak and keep the supply line liquid nitrogen from generating vapor. The returning flow is vaporized with a heater, followed by a flowmeter to monitor flow through the cathode. A machine protection interlock is provided by this flowmeter when the flow stops through the cathode head.

SRF Gun Cryostat

A 150 liter reservoir, located above the gun cavity, allows the system to operate for a while without filling with liquid helium from the cryogenic system. This will allow the subatmospheric pump to handle the maximum heat load when required. 5 intercept circuits flows, using 3 bar liquid helium to intercept the two beam tube flanges, the two fundamental power coupler outer conductors, and the HTS solenoid are returned after warming to room temperature using electric heaters, to each thermal mass flow controller located outside the radiation blockhouse. The cryostat also has a liquid nitrogen cooled shield thst surround the cavity and helium reservoir.

The expected loads and consumption of the system follows below.

Liquid nitrogen consumption 5 Cell Cavity/Ballast Tank, 14 LPH; SCRF Gun, 6 LPH; Gun Cathode, 20 LPH when powered; 1660S Coldbox, 70 LPH

2 K liquid helium heat load 5-cell cavity, 6 W static, 40 W dynamic; 5-cell LHe reservoir, 2 W; 5-cell J-T valve, 6 W; Gun cavity, static 8 W, dynamic 7 W; Gun LHe reservoir, 3 W; Gun J-T valve, 3 W

5 K, 3 Bar LHe flow 5-cell cavity FPC, 0.075 g/s; 5-cell beamtube transitions, 2 x 0.075 g/s; Gun end flanges 2x 0.075 g/s and solenoid, 0.075 g/s; Gun FPC 2 x 0.075 g/s.

With a 2K load of at least 75 W, the vacuum pump flow will be 4.3 g/s, and with approximately 0.8 g/s liquefaction load from the intercepts, the total liquefaction demand load is 5.1 g/s, which is higher than the net 3.0 g/s liquefaction capacity of the plant. The additional 2.1 g/s capacity will come from the low pressure storage dewar, using the subcooler as the transfer device.

With 2000 liters reserve, the system can operate 24 hours, before stopping. If the cavities operate at the full capacity of the vacuum pump, 5.5 g/s, then the total demand is 6.3 g/s. The run time becomes 16 hours.

Reliquefaction of the equivalent of 2000 liquid liters from warn storage while keeping the cavities cold at 4.5K requires 50 hours.

1.1.2.7 *Magnets and optics*

One of the critical parts of the ERL is the merger of the low-energy - and high-energy beams.The injection energy is not recovered. A low injection energy requires less RF power and lowers dumped beam energy. The original emittance compensation scheme does not include any dipoles between RF gun and linac (or booster cavity). In the R&D ERL the novel emittance preserved merger system will be tested for the first time. As a result of beam dynamics simulation the R&D ERL injector is expected to provide electron beam 0.7 nC of charge and equal normalized emittances in vertical and horizontal planes 1.4 mm-mrad [9].

The lattice of the ERL loop controls the parameters of a symplectic transport matrix, which affect the stability and operation conditions of the ERL. The lattice of the loop is intentionally chosen to be very flexible for the R&D ERL to be a test-bed of new ampere-range of beam currents in ERL technology. The adjustable part of the lattice has two arcs and a straight section. Each arc is an achromatic with adjustable longitudinal dispersion value from +1 m to -1 m. Quadrupoles in the dispersion-free straight section provides for matching of the end quadrupoles. These quadrupoles will be used for conducting the transverse beam break up studies. The simulation for normal operation of R&D ERL shown that BBU threshold current is in the level of 20 A.

In order to change the returning path length one of the 180 degrees arc is movable to/from the main Linac by 1/8 of RF wavelength (6 cm). By changing the path length ERL can operate in: normal CW energy recovery mode as well as more exotic modes: double acceleration and three passes through the Linac. More details about R&D ERL optics can be found [10].

The return loop magnets are of traditional design with the following exceptions:

a) The bending radius of the 60^o dipole magnets is 20 cm, which is rather small. We use 15^o edges on both sides of the dipoles to split the very strong focusing evenly between the horizontal and vertical planes (so-called chevron-magnet).

b) The requirements on field quality of the loop's quadrupoles had been determined by the requirement to preserve a very low normalized transverse slice emittance of electron beam (ε_n~ 1mm-mrad). We used direct tracking of a sample electron beam to verify a high degree of the emittance preservation.

c) Each quadrupole is equipped with a dipole trim coil, which can be also used to excite a sextupole component, if required, for emittance preservation of e-beam with a large energy spread.

One of the unique features of all ERLs is the necessity for merging low and high-energy electron beams. In the R&D ERL, 2 MeV from the SRF gun merges with the 20 MeV

electron beam coming around the return loop into the same trajectory at a position within the SRF linac. In the linac, injected bunch is accelerated to 20 MeV, while the returned or "used" bunch is decelerated to 2 MeV. The challenge for a merger design is to provide conditions for emittance compensation and also for achromatic conditions of a low energy, space-charge dominated electron beam. The scheme that satisfies these requirements (called Z-bend) is used on the R&D ERL [9]. The Z-bend is approximately 4-meter long. It bends the beam trajectory in the vertical plane. It is comprised of four dipole magnets designed to be equally focusing in both planes, with bending radius ~ 60 cm, and bending angles of: $+15^o$, -30^o, $+30^o$ and -15^o. The beam dynamics in the Z-bend results in a large-size (centimeters) near-laminar electron beam.
The large beam size and very low slice emittance of the e-beam dictates the tolerances on the magnetic field to be very tight. The integrated nonlinear kicks should not exceed ~20 micro-radian per magnet at a typical radius ~ 1 cm. The magnets in the Z-bend are rather short (15 cm effective length for the 15^o magnet) and have a rather large aperture of 6 cm. Analysis predicts that the influence of various field components on the emittance growth are complicated by the fact that the beam trajectory bends significantly in the fringe fields. Hence, we decided to use direct tracking in the calculated fields extracted from Opera3d of test beam to evaluate and to minimize influence of magnetic field on the beam emittance.
All R&D ERL magnets were designed using Opera3d for 3D magnetic field calculations as well as the influence of geometric tolerances on the field quality [11].
All four dipole magnets (15 and 30 degree) used at the merger have a rather complex window-frame design with parallel edges, constructed with four coil sets (vertical dipole, main quadrupole, small sextupole coils in the corner, and horizontal correction dipole, wound with the quadrupole coils). The quadrupole coil is used to split the focusing strength equally between the planes, while the main dipole coil is designed to create both dipole and sextupole components of the field which is necessary for emittance preservation. The amount of the sextupole component is controlled by the gap between the yoke and the main dipole coil. A small additional coil in the corners is a sextupole trim coil. Magnetic measurements of the ERL magnets employed both rotating coil and Hall probe array mapping.
The Hall probe array comprises of four Group3 Hall probes spaced by 10 mm. The relative centers of the probes are measured in a quadrupole with accuracy of a few micrometers. The hall probe array is calibrated against an NMR probe in a test dipole. Overall accuracy of the magnetic field measurements is ~ 0.03%, while relative accuracy of the rotating coil measurements is better than 50 ppm.
We used direct tracking of 2,000 particles in the 3D magnetic field, which calculated by Opera3d/Tosca. For the Z-chicane dipoles we used initial distribution of electron with kinetic energy of 2.77 MeV and transverse radius of 1 cm. These particles were tracked from the center of the magnet to far (0.5 m to be exact) outside the magnet using Opera-3d Post-processor with the step of 1 mm. The output file contains all 3D position and velocity components at each step. Another program was used to translate these components to a local coordinate system, which was defined by the final position and momentum of the central ray. These results led to the extraction of the final phase space distribution (x, x', y, y'). This data was then analyzed using various programs and the next iteration of the magnet design was processed.
One of the tools used was the expansion of angles of the trajectory (x',y')out far from the magnet exit as function of initial coordinates (x,y)in. Since the trajectories are

strongly curved, these expansions do not have clear harmonic content (for example x2 and y2 terms have different coefficients). Therefore we had used the increase of the beam emittance as a figure of merit, while using coefficients in second and third order expansions as guidance.

All the ERL magnets are accurately CNC machined and installed on similarly machined bases. Within each base there is no provision for alignment, the CNC machining achieves tolerances better than a survey procedure.
A portion of the ring is mounted on a movable gantry with a total stroke of 10 cm, to allow phasing of the return beam to various values.
The Ring Arc Dipoles gap is 3 cm with a central field of 3.3 kGauss. The magnetic length is around 19 cm with a field quality of sextupole b3 to dipole integral ratio approximately equal to $1.2x10^{-4}$ at a radius equal to 1 cm and the quadrupole ratio required is about 2.1%.
The Ring Quadrupoles have a required gradient of 0.3 kGauss/cm. Pole diameter aperture is 6 cm, with a tip field of approximately 900 G and magnetic length of about 16 cm. The field quality 12-pole integral ratio is $1.6x10^{-4}$ at a radius of 2.5 cm.
The injection 30-degree z-bend Dipole/Quad combined magnet has a half-gap of 3.644 cm and is designed to minimize the b3 sextupole component. The central field is 191.3 G with a magnetic length of approximately 29.6 cm. The field quality has an integrated sextupole ratio of 4E-4 and octupole ratio of $3x10^{-4}$ at a radius of 1.5 cm.
The injection 15-degree z-bend Dipole/Quad combined magnet has a half-gap of 3.544 cm and is designed to minimize the b3 sextupole component. The central field is 145.1 G with a magnetic length of approximately 19.2 cm. The field quality has an integrated sextupole ratio of $2.3x10^{-4}$ and an octupole ratio of $1.3x10^{-4}$ at a radius of R=1.5 cm.
The solenoid pair is designed with a peak field of 984 G, assuming a separation of 5 inches steel to steel or 9.5 inches center to center. Maximum coil current is 8.4 amps at a maximum voltage of 13.4 volts.
The Quadrupole Doublet used in the arc has a required field gradient of 58 Gauss/cm. The field quality, assuming all coils are powered, has an integrated octupole ratio of $5.3x10^{-4}$ and a 12-pole ratio of $4.1x10^{-4}$.

1.1.2.8 ***Power supplies***

The magnet assemblies used in the ERL consist of one or more windings on a common core. Each of the windings represents a separate magnet load for the power supply. As the ERL is operated in a DC fashion, interaction between the windings is not a concern.
Appendix A lists all the magnet assemblies by sector. Each coil is listed by name and model. The model corresponds to a set of electrical and magnet parameters as established by the magnet subsystem.
Some of the coils are connected in series. The connection scheme, plus cabling provides the electrical load characteristics. The load information, plus the operating current, and the stability define the power supply requirements.
Five different models can satisfy all of the magnet power supplies requirements for the ERL. The capsule specifications and quantities are listed below:
One IE Power model UD320A35V, 35V, 320A, 100 ppm
Thirty four Danfysik Shim Amplifier 892, 15V,10A, 100ppm
Five Kepco model BOP 50-20GL, 50V, 20A, 100ppm

Thirty two BiRa model MCOR12 / 2A, 25V, 2A, 1000ppm
Six BiRa model MCOR12 / 6A, 25V, 6A, 1000ppm
With the exception of the UD320A35V unit, all models are bipolar, even though not all loads require bipolar operation. But, by using standard off-the-shelf units, development costs were minimized.

1.1.2.9 ***Vacuum***

The ERL has a number of vacuum volumes with various sets of requirements. These are the Superconducting RF Cavity, Superconducting electron-gun, injection region, ERL loop, beam dump and laser transport line.
The beamline vacuum regions are separated by electro-pneumatic gate valves. The beam dump is common with loop beamline but is considered a separate volume due to geometry and requirements. Vacuum in the 5-cell SRF cavity is maintained in the ~10^{-9} torr range at room temperature by two 20 l/s ion pumps and in the electron-gun SRF cavity by one 60 l/s ion pump. Vacuum in the SRF cavities operated at 2ºK is reduced to low 10^{-11} torr via cryopumping of the cavity walls. The cathode of the electron-gun must be protected from poisoning, which can occur if vacuum adjacent to the electron-gun in the injection line exceeds 10^{-11} torr range in the injection warm beamline near the electron-gun exit. The vacuum requirements for beam operation in the loop and beam dump are 10^{-9} torr range. The beamlines are evacuated from atmospheric pressure to high vacuum level with a particulate free, oil free turbo-molecular pumping cart. 25 l/s shielded ion pumps distributed throughout the beamlines maintain the vacuum requirement. Due to the more demanding vacuum requirement of the injection beamline proximity to the electron-gun, a vacuum bakeout of the injection beamline is required. In addition, two 200 l/s diode ion pumps and supplemental pumping provided by titanium sublimation pumps are installed in the injection line just beyond the exit of the electron-gun. Due to expected gas load a similar pumping arrangement is applied at the beam dump. The cryostat vacuum thermally insulating the SRF cavities need only reduce the convective heat load such that heat loss is primarily radiation through several layers of multi-layer insulation and conductive end-losses which are contained by 5ºK thermal transitions. Prior to cool down rough vacuum ~10^{-5} torr range is established and maintained by a dedicated turbomolecular pump station. Cryopumping by the cold mass and heat shields reduces the insulating vacuum to 10^{-7} torr range after cool down.
The superconducting cavities are processed in particulate free environments to achieve the highest gradient possible. Particulates must also be eliminated from adjacent components of the injection and loop beamlines to avoid particulate migration into the SRF cavities. The particulate free requirement of beamline components represents the most challenging aspect to meeting the beamline vacuum requirements. A significant effort is focused on developing particulate free capability. Procedures and an on-site clean room processing facility at BNL were developed for processing new beamline components and QA of particulate processed components supplied by outside sources.
The laser beam travels from the laser room to the photocathode through a transport line consisting of evacuated tube sections and a series of mirrors and lenses prior to entering the ERL injection beamline. Laser transport vacuum is established with a mechanical pump, maintained with a small ion pump and monitored with a vacuum gauge.
Pressure relief to protect both personnel and equipment has been incorporated into the warm and superconducting beamlines to meet the requirements of Section VIII of the Pressure Vessel and Boiler Code. Relief devices include spring-loaded plates for

cryostats and burst diaphragms for the beamlines. The SRF pressure relief devices are installed on the warm ends of the SRF strings. Cryostat and SRF beamlines relief devices are plumbed into vent headers to prevent an Oxygen Deficiency Hazard (ODH) condition in the ERL experimental area. Burst diaphragms installed on warm beamlines are vented directly into the experimental area because failure modes and conditions indicate an ODH 0 level can be maintained and the complexity of routing extra vent headers can be avoided.

The electron loop environment is entirely room temperature. The beamline is composed of dipole and quadrupole magnet chambers, drift chambers and various beamline components. Vacuum components include ion pumps, gauges and valves. All magnet chambers are made from non-magnetic materials to adhere to the strict magnetic field requirements. Dipole magnet chambers are made from aluminum. Ease of machining and low outgassing rates when processed properly are added benefits of using aluminum. Results of outgassing measurements performed with a baked 1st article aluminum dipole chamber reveal rates of low 10^{-12} torr·liter/sec·cm2. This result compares favorably with clean, baked stainless steel material. The dipole chambers were built by Atlas Technologies.

Dipole chambers are machined as half cores and externally welded together. The weld is not full penetration to keep the chamber inner surface smooth. The proprietary weld prep maintains a smooth chamber ID profile without trapping volume. Atlas explosion bonded bimetal Conflat type flanges are welded to the chamber assembly allowing standard Conflat gasket and hardware to interconnect mating beamline components.

Chambers passing through quadrupoles are made from inconel tube. The magnetic permeability of the quad chamber inconel beam tubes is less than 1.01. The remainder of the quadrupole chamber is made from 304L stainless steel. Hydroformed bellows that form part of each quadrupole chamber are made from inconel. The quadrupole chambers were built by MDC.

Vacuum gauging and pumps are all mounted on crosses at the end of quadrupole beampipes. In addition button beam position monitor (BPM) cubes are integrated with the quadrupole chambers. BPM buttons are installed in the cubes. The BPM cube incorporates the primary chamber mount. The cube dimensions are controlled to very tight tolerances for positioning the BPM buttons such that beam based alignment techniques are not required. The dipoles quadrupoles and associated beam pipe supports are pinned to a tight-tolerance strong back to insure the precision of the BPM buttons to the magnets and beam centerline.

A basic assembly of magnets and chambers installed on a strong back otherwise known as a triplet assembly (3 quads and a single dipole) is used as a unit in the ERL loop. A few other basic units are also used. All the components are fabricated to a high tolerance and mounted to precision milled positions on a single support plate. The chambers are interconnected with 4-1/2 inch Conflat type flanges. The cross ports for gauging and beam components are either 2-3/4 inch or 4-1/2 inch Conflat flanges.

The BPM buttons are sealed to the BPM cube with Helicoflex delta seals. The seal groove is machined into a mini-Conflat (1.33 inch) bolt circle. The sealing force, less than a comparable Conflat seal, insures an even metal-to-metal interface between button and cube. This lower compressive force seal helps maintain the precision placement of the button relative to the beam centerline with more uniform contact between the machined face of the BPM cube and that of the BPM button flange. The seal has an aluminum jacket that limits bakeout temperature to 150ºC.

Components destined for the ERL beamline are either delivered to BNL or processed at BNL for suitability of service in an ISO 14644 Class 5 clean room. This processing includes vacuum flange seals and hardware. Components delivered Class 5 ready are double bagged and are only opened in a Class 5 environment. All QA is performed in the class 5 environment. If QA outside the Class 5 environment is needed, then re-processing for particulate free service is needed. So, careful attention and coordination is needed to avoid costly re-work if at all possible.
In case helium processing of the SRF cavities is desired, a helium introduction system was installed on the beam line. Research grade 99.9999% helium is passed through a purifier and 0.003 micron filter before being introduced to the cavity through a all metal variable leak. This system requires local access to the cavity for adjustments in pressure. The helium system is remote operational by controlling the variable leak with Selsyn (self synchronous) motors.

1.1.2.10 ***Beam Instrumentation***

A variety of beam instrumentation systems will be provided for the purpose of commissioning, tuning, and protecting the ERL facility. Measurements that include beam position, profiles, current, emittance, and losses will be available for the planned modes of operation [12].

1.1.2.10.1 Beam Position Monitors

There are 16 dual plane 10mm diameter button style Beam Position Monitors (BPMs), 4 in the injection transport, 11 in the recirculation loop, and 1 in the dump line. The buttons are Times Microwave Systems model SK-59044; they are mounted on stainless cubes that are welded to the adjacent 6cm diameter beam pipes. The orientation of the cubes are installed either at 45^0 or 90^0 depending on their location. A 45^0 orientation is used if there are space limitations, and to avoid beam related energy deposition on a button downstream of bending magnets. The BPMs will be baked to 150C.
Libera Brilliance Single Pass electronics from Instrumentation Technologies will process signals from the BPMs. These modules have been customized with a 700MHz SAW band pass filter that matches the fundamental frequency of the SCRF gun and Linac accelerating cavities. A few fundamental characteristics of the Libera system are that it employs a digitizer with a 117MHz-sampling rate, a variable buffer length of 1k–8kB, a maximum trigger rate of 200Hz, and position threshold comparison beam inhibit output for machine protection. BPM signals will be transported to the signal processing electronics using Andrew LDF1-50 1/4” heliax cable to preserve the signal power at the 700MHz Libera pass band. When operating with typical ERL bunch trains of 9.3MHz, 351MHz, or 703MHz, performance parameters should be compatible according to simulations. Since the spacing between bunches in a bunch train will be ~100ns or less, and the 700MHz filter will ring for >100ns, the individual bunch position will be difficult to distinguish within bunch trains. The configurable beam position range interlock feature offered by the Libera electronics will be employed as the first line of defense for machine protection and to avoid beam losses.
The Libera BPM electronic units will be integrated into the standard RHIC control system. ADO (accelerator device object) software has been written and will execute directly on the Linux kernel that is resident in the Libera hardware. The ADO provides on-board communication to the Libera hardware through the CSPI (control system

programming interface) library provided by I-Tech, and communicates to higher level workstations via Ethernet using standard RHIC control system utilities.

1.1.2.10.2 Beam Profile Monitors

Transverse beam profiles will be measured by two methods, depending on the amount of beam charge in the bunch train. When in low charge operating mode with 1-100pC bunch charge trains, we will use 0.1 X 50mm YAG:Ce (yttrium aluminum garnet doped with Cerium) screens from Crytur (40mm clear aperture). For higher charge modes we will use OTR (optical transition radiation) screens that are comprised of a 250micron thick silicon wafer coated with ~1000 angstroms of aluminum. The profile monitor stations were specified by BNL and designed and fabricated by Radiabeam Technologies. Images from the YAG and OTR screens are transported through a mirror labyrinth to a 3-motor lens and CCD camera in a local enclosed optics box. We plan using our ERL Linux Red Hat Controls [C] interface to a Grasshopper2 GigE camera.

A more simplified YAG profile monitor has been designed to plunge into the beam path of the injection 30^0 dipole chambers through an auxiliary port.

Synchrotron light monitors will be used to measure transverse beam profiles while running with high power beams. Due to the long wavelength of synchrotron radiation at 20MeV, and low sensitivity of CCD cameras at these wavelengths, using these monitors could be challenging. We plan to install optical transports and CCD cameras at a number of the ERL loop 60^0 dipole locations. The dipole chambers have dedicated synchrotron light output viewing ports.

Halo scrapers will be installed in the injection transport to measure the amount of beam in the halo. Horizontal and vertical pairs of stepper motor controlled 2mm thick copper jaws will be located at several locations in the injection transport. After the halo characteristics are measured, a collimator will be designed to scrape off the undesired halo at low energy to reduce higher power beam losses downstream.

1.1.2.10.3 Beam Emittance

There are two techniques planned to measure beam emittance. The expected normalized emittance range is 2-10um.
In the first method, a pepper pot station will be used to measure 2MeV beam emittance in the injection transport. The pepper pot will be comprised of two plunging tungsten masks upstream of a YAG:Ce profile monitor, one located at 0.25m, and the other 0.5m. The dynamic range of the emittance measurement will be limited by the space charge effect. The space charge effect can be characterized by the ratio of the space charge and emittance contribution in the beam envelope equation.
The second method will measure the 20MeV Beam emittance will be measured using the
traditional quad scan technique, and image data from downstream YAG & OTR profile monitors.

1.1.2.10.4 Beam Current Monitors

High precision DC current measurements will be made using a matched set of Bergoz NPCT-S-115 DC current transformers (DCCT) and standard NPCT electronics.

There will be one each installed in the injection and extraction transport beam lines. These DCCTs are configured in a nulling mode where their calibration windings are joined in a single loop, and driven opposite the beam by a low-noise Khronhite model 523 current source. The output level of the dump DCCT is fed back as a reference to the current source to drive the dump DCCT output to zero. The output of the gun DCCT is then a differential current measurement [13].
We are presently considering several signal processing and data analysis hardware solutions from National Instruments for handling DCCT system tasks that include absolute and differential measurements. Drift (magnetic field, thermal, and gain) compensation will be automatically removed by periodic nulling without beam.
The anticipated sub-microamp resolution may permit using this diagnostic as a second layer of the machine protection system in the case the beam loss monitors fail to detect beam losses.
Bunch-by-bunch & bunch train charge will be measured by a Bergoz in-flange Integrating Current Transformer (ICT) part number ICT-CF6-60.4-070-05:1-H-UHVTHERMOE, located in the upstream injection line. This ICT assembly has internal type E thermocouple for bake out (to 150C) temperature monitoring..
Beam charge signals will be processed by standard Bergoz BCM-IHR Integrate-Hold-Reset electronics feeding a beam synched triggered digitizer. The nominal integrating window is 4us, but can be adjusted shorter or longer based on the temporal limits of the electronics.We have ordered the BCM-IHR module with the option to trigger at a maximum frequency of 10kHz.

1.1.2.10.5 Beam Loss Monitors

Photomultiplier tube (PMT) based loss detectors will be installed at locations where beam loss is most likely. The design of this detector is based on ones developed at Jefferson Lab, they using the Burle 931B PMT; a more modern tube was chosen for ERL. The Hamamatsu R11558 side-on tube is very similar to the 931B and has lower dark current, higher gain, and improved anode and cathode responsivity. The PMT was installed in light tight PVC housing containing a 10mA green LED for testing with 1μS light pulses. In an effort to extend the use of the existing RHIC BLM System [14] processing electronics to the ERL, a preprocessing VME module had to be designed. As the RHIC BLM front-end V119 typically takes loss signals from positively biased ion chambers, the characteristically negative signal from the PMTs had to be inverted. Thus a custom interface for the VME chassis was developed containing eight independent channels of inverting amplifiers with integration matching that of the V119 card, and having an output stage for driving the capacitive input of the V119 card. A maximum gain of 200 was demonstrated with good signal to noise ratio. The interlock response time to a loss signal that exceeds a programmable threshold is ~10μs. The actual PMT gain at each location will be field adjusted by setting the high voltage bias during beam commissioning. A CAEN HV multi-channel chassis with full remote control will bias the PMTs.
Eight Ion Chamber (IC) loss detectors, as currently used in RHIC, will be employed at select locations in ERL. These are 113cc glass bottles with BNC & SHV connectors for signal and bias. These will be collectively biased to 1400V in two groups by two Bertan 205B-03R 3kV 10mA rack mount power supplies. The signals from each IC are transported on 75 ohm cables to the V119 modules. All V119 modules (PMT and IC connected) are supervised by a V118 module that monitors integrated signal level data

compared to thresholds. The V118 module has a discrete loss output signal that will signal the machine protection system in the event of detected loss from any of the PMTs or ICs.
Ion chamber type loss monitors based on gas filled heliax cable, as used in the AGS ring, will be employed at ERL. The cable is 7/8 inch heliax, Andrews type RG318, filled with Argon to 10 psig. Four long loss monitor cables will run along the inside of the loop while 12 short loss monitor cables will hug the outer casing of the final beam dump. The cable loss monitors are biased to ~150V by custom floating bias supplies mounted in NIM modules. The loss signal returns on the bias cable and is integrated by a custom integrating amplifier modules whose analog outputs are digitized by standard VME DAC modules.
In addition to amplitude proportional beam loss detection as provided from the PMT, IC, & heliax detectors, event count based detectors are employed. PIN Diode loss detector modules, Bergoz model BLM, will be installed at eight select locations in ERL. These modules are built around two PIN photodiodes mounted face-to-face making use of coincidence counting to be insensitive to synchrotron radiation photons. With extremely low spurious count rate of < 1 in 10 sec, up to 10 MHz counting, dynamic range of 10^8, and 100nS recovery time, these detectors are of the lowest costs and highest dynamic ranges available. The TTL data output of each detector is counted by a Struck model SIS3808 scalar VME module.
Thermal imagers will be used at several locations to measure beam pipe temperature gradients to ensure beam losses not seen by other loss detectors are monitored. We chose the FLIR A310 camera. It offers image transfer and control via Ethernet, and configurable location specific temperature thresholds on the image can be programmed and used to provide a machine protection alarm or interlock signal from a digital output port on the camera assembly.

1.1.2.11 ***Beam Dump***

We use a commercially available beam dump modified to the ERL special needs. The beam dump design is based on a similar 1 MW ERL klystron electron gun beam dump from CPI, which was purchased a few years ago. However, that and other similar commercially available MW beam dumps were designed to remove 10's of Ampere beams with energies of 10's of KeV. Therefore, upon entry into the beam dump, the electron beams spread out due to their high space charge and relatively low energies.
However for the ERL parameters, the beam dump has to address the issues of cascade showers, forced magnetic beam spreading due to low space charge at high energy, and issues associated with extremely high radiation doses. Therefore, a beam modified beam dump was designed and a purchased order was sent to CPI. Beam spreading is to be done magnetically to address the first two issues. All elastomer seals are to be replaced by metallic seals, or flanges are to be welded. Dimensions of this beam dump are roughly 62" in length and 19" in diameter. Spreading the beam over this large area is to ensure that local boiling of the cooling water does not occur. The beam will be spread over this large surface area by magnetic field coils. Elastomer seals, which are replaced by welding flanges, have a 1" lip in order to facilitate easy opening, even though it is very unlikely that such a need will arise. To mitigate debris and outgassing streaming back into the rest of the ERL system, the inner copper walls of the beam dump are to be conditioned at low power without cooling; backscattering, secondary

electrons etc. are not an issue due to the fact that the electron beams striking the inner copper walls have multi-MeV, and thus penetrate deeply into the walls.
The beam dump is designed to have the capability for removing 1 MW of unrecovered electron beam power with beam energy of 5 MeV. Similar design with identical heat removing capability was successfully tested at 1.6 MW.

1.1.2.12 *Control System*

1.1.2.12.1 Machine Protection System

The Machine Protection System (MPS) is a device-safety system that is designed to prevent damage to hardware by generating interlocks, based upon the state of input signals generated by selected sub-system. It exists to protect key machinery such as the 50 kW and 1 MW RF Systems. When a fault state occurs, the MPS is capable of responding with an interlock signal within several microseconds. The Machine Protection System inputs are designed to be fail-safe. In addition, all fault conditions are latched and time-stamped.
The ERL MPS is based on a National Instruments hardware platform, and is programmed by utilizing National Instruments' development environment for a visual programming language. The MPS runs on a programmable automation controller called CompactRIO (Compact Reconfigurable Input Output). The National Instruments CompactRIO is an advanced embedded control and data acquisition system designed for applications that require high performance and reliability. This small sized, rugged system has an open, embedded architecture, which allows developers to build custom embedded systems in a short time frame. The National Instruments CompactRIO device that is used for the MPS is an NI cRIO 9074. The cRIO 9074 is an 8-slot chassis with an integrated real-time processor and an FPGA. The embedded real-time processor is a 400 MHz Freescale MPC5200 that runs the WindRiver VxWorks real-time operating system. The FPGA is a Xilinx Spartan 3 with 2 million gates (46,080 logic cells) and 720 KB embedded RAM. The cRIO 9074 also features a 256 MB nonvolatile memory. CompactRIO combines an embedded real-time processor, a high-performance FPGA and hot-swappable I/O modules to form a complete control system. Each module is connected directly to the FPGA and the FPGA is connected to the real-time processor via a high-speed PCI bus.
ERL critical sub-systems such as the RF system require the MPS to respond on a microsecond scale. High-speed I/O modules were chosen to meet the necessary timing requirements. The MPS currently uses three of these I/O modules: a 32-channel 24V input module, an 8-channel TTL input-output module, and a 4-channel SPST relay output module. The 24V module has sinking digital inputs with 7 μs response time, and the TTL module has digital inputs and outputs with 100 ns response time.
The MPS interface is written in LabVIEW (Laboratory Virtual Instrumentation Engineering Workbench). LabVIEW is a graphical programming environment used to develop measurement, test, and control systems utilizing graphical icons and wires that resemble a flowchart. The National Instruments CompactRIO platform requires two different LabVIEW software modules corresponding to the System's interface, one for the Real-Time processor and one for the FPGA. These modules contain custom functions specific to the Real-Time processor or the FPGA in addition to all the functionalities of the standard LabVIEW module.

The code for both the Real-Time processor and the FPGA is developed on a host computer. The program for the FPGA is developed by using a standard LabVIEW software module. The LabVIEW FPGA code is then converted to VHDL code and compiled using the Xilinx tool chain. The program for the Real-Time processor is also developed by using a standard LabVIEW software module. When ready, the code for the Real-Time processor and the FPGA is downloaded to the CompactRIO device via Ethernet. Once the code is downloaded, the CompactRIO can run in a stand-alone mode, or communicate directly with a host via Ethernet.
Running directly on the cRIO platform, the MPS interface accepts the various input signals and generates any necessary interlocks. An interlock is generated when a logic high (fault) at the input is seen. (If a cable is disconnected or broken, an internal pull-up ensures the System will generate an interlock. Exception is given to the RF sub-system which provides high-level inputs due to equipment constraints. These inputs are inverted within the LabVIEW FPGA.) If one of the continuously polled input levels change to high (indicating a fault), the fault is latched, and the time of the event is recorded using a 32-bit LabVIEW tick counter function. This provides a microsecond time stamp. The MPS interface also provides the capability to enable and disable inputs. Enabled and latched inputs are then combined and passed to other critical systems as interlocks. The input latches are cleared only after a software reset has been issued.
Operators communicate to the MPS interface using the main ERL server. Operators have the ability to enable/disable individual system inputs, clear latches via a reset button, and check the overall system status. The Real-Time processor code performs a handshake with the main server to ensure connectivity. National Instruments also provides web server capability, which allows the developer to monitor and control the system remotely, avoiding interaction with the ERL main server.

1.1.2.12.2 Infrastructure for the control system

The control system runs on server PC's running Red Hat LINUX, with one being dedicated to laser-related activities.
End-user access to the ERL controls system is handled by three Wyse thin-client terminals located in the Control Room. Each terminal has the capability of connecting via Ethernet to three different remote hosts that are running as No Machine servers, and can drive up to two separate video displays.
Three VME chassis running VxWorks on multiple processor platforms are used to support remote device integration with the controls system. Remote diagnostics are also available for each unit via RS-232 connections. Continuous time synchronization between all chassis and a networked timeserver is achieved using Extended Network Time Protocol (XNTP).
RS-232 and 485 serial connections are integrated with the controls system Ethernet network using several different types of Digi Terminal Server modules.
All GPIB interface devices are integrated with the controls system Ethernet network using National Instruments GPIB/ENET-100 modules.
Commonly used application software within the Collider-Accelerator Complex for device interaction (PET), live-information plotting (GPM), logged-information plotting (LogView), and video image display/analysis (FlagProfileMonitor) will continue to serve has the primary controls system tools for the ERL project. Motif Editor and

Display Manager (MEDM) will be used to create synoptic displays that will eventually provide the primary user interface to the ERL.
A 100 Megabit Ethernet network serves as the backbone of the controls system. Dedicated Gigabit Ethernet links will likely be needed in support of selected high-frame rate video connections between video servers and the ERL Control Room.
Data logging services are provided by a set of networked servers shared by other projects at the Collider-Accelerator Complex. Each machine utilizes RAID storage in order to maintain a high level of reliability.

1.1.2.13 *Summary, Status and Plans*

We provided a detailed description of the design of the various subsystems of the R&D ERL which is in advanced construction and commissioning at the Collider-Accelerator Department at Brookhaven National Laboratory. At the time of writing of this manuscript, all elements of the ERL are in house and most are installed and surveyed to their exact positions. The first beam from the SRF gun is expected in October 2012, beam through the 5-cell cavity is anticipated in December 2012 and beam through the ERL loop in March 2013. We plan to study the performance of this unique machine: The high QE photocathodes and their load-lock delivery system, the SRF gun capable of 500mA current at 2MeV beam kinetic energy, the zig-zag beam merger, the highly damped 5-cell SRF accelerating cavity, and various advanced instrumentation elements. Of particular interest are the high-current, low-emittance properties of the system, like coherent emissions, beam halo evolution and mitigation and emittance preservation. We plan to increase the current gradually from sub-mA to ampere-class in stages.

This article has been authored by employees of Brookhaven Science Associates, LLC under Contract No. DE-AC02-98CH10886 with the U.S. Department of Energy. The United States Government retains a non-exclusive, paid-up irrevocable, world-wide license to publish or reproduce the published form of this article, or allow others to do so, for the United States Government purposes.

1.1.3 **References**

1. T. Vecchione, I. Ben-Zvi, D. H. Dowell, J. Feng, T. Rao, J. Smedley, W. Wan, and H. A. Padmore, A Low Emittance and High Efficiency Visible Light Photocathode for High Brightness Accelerator-Based X-ray Light Sources, Appl. Phys. Lett. **99**, 034103 (2011)
2. Diamond amplified photocathode references:
    a. BNL Collider-Accelerator Department note C-A/AP/149 04/04 Secondary Emission Enhanced Photoinjector, I. Ben-Zvi, X. Chang, P. D. Johnson, J. Kewisch, T. S. Rao, 2004
    b. Xiangyun Chang, Ilan Ben-Zvi, Triveni Rao, John Smedley, Erdong Wang, Qiong Wu, Tianmu Xin, Neutralizing trapped electrons on the hydrogenated surface of a diamond amplifier, Phys. Rev. ST Accel. Beams 15, 013501 (2012)
    c. Erdong Wang, Ilan Ben-Zvi, Triveni Rao, D.A.Dimitrov, Xiangyun Chang, Qiong Wu, Tianmu Xin, Secondary-electron emission from hydrogen-terminated diamond: Experiments and model, Phys. Rev. ST Accel. Beams 14, 111301 (2011)

   d. Erdong Wang, Ilan Ben-Zvi, Xiangyun Chang, Qiong Wu, Triveni Rao, John Smedley, Jorg Kewisch, and Tianmu Xin, Systematic study of hydrogenation in a diamond amplifier, Phys. Rev. ST Accel. Beams **14**, 061302 (2011)
   e. D. A. Dimitrov, R. Busby, J. R. Cary, I. Ben-Zvi, T. Rao, J. Smedley, X. Chang, J. W. Keister, Q. Wu, and E. Muller, Multiscale three-dimensional simulations of charge gain and transport in diamond, Journal of Applied Physics **108**, 073712 (2010)
   f. X. Chang, Q. Wu, I. Ben-Zvi, A. Burril, J. Kewisch, T. Rao, J. Smedley, E. Wang, E. M. Muller, R. Busby, and D. A. Dimitrov, Electron Beam Emission from a Diamond-Amplified Cathodes, Physical Review Letters **105**, 164801 (2010)
3. E. Pozdeyev, et al, "Diagnostics of the BNL ERL", PAC2007, pg. 4387, FRPMS116
4. A.K. Sharma, T. Tsang, and T. Rao; Theoretical and Experimental Study of Passive Spatio-Temporal Shaping of Picosecond Laser Pulses; BNL 81555-2008JA; Phys. Rev. Special Topics 12, 033501 (2009)
5. R. Calaga, I. Ben-Zvi, M. Blaskiewicz, X. Chang, D. Kayran and V. Litvinenko, High current superconducting gun at 703.75 MHz , Physica C: Superconductivity, **441**, 159, (2006)
6. Wencan Xu, et al, Design, Simulation and Conditioning of the Fundamental Power Couplers for BNL SRF Gun, Proceedings International Particle Accelerator Conference IPAC12, New Orleans USA, WEPPC114.
7. R. Gupta, et al, Design Construction and Test Results of a HTS Solenoid for Energy Recovery Linac, Proceedings of 2011 Particle Accelerator Conference, New York, NY, USA, TUP163
8. H. Hahn, I. Ben-Zvi, R. Calaga, L. Hammons, E. C. Johnson, J. Kewisch, V. N. Litvinenko, and Wencan Xu, Higher-order-mode absorbers for energy recovery linac cryomodules at Brookhaven National Laboratory, Phys. Rev. ST Accel. Beams **13**, 121002 (2010).
9. D. Kayran, V.N. Litvinenko, Merger system optimization in BNL's high current R&D ERL. Proceedings of PAC'07, pp. 3711-3713.
10. D. Kayran et al, Optics for High Brightness and High Current ERL Project at BNL, in Proceedings of PAC 2005, pp. 1775-1777.
11. W. Meng, A. Jain, G. Ganetis, D. Kayran, V.N. Litvinenko, C. Longo, G. Mahler, E. Pozdeyev, and J. Tuozzolo, *Unique Features in Magnet Designs for R&D Energy Recovery LINAC at BNL*, Proceedings of PAC07, Albuquerque, New Mexico, USA, p. 655-7.
12. David Gassner, Dmitry Kayran, Leonard DeSanto, Chuyu Liu, George Mahler, Rob Michnoff, Toby Miller, Michelle Wilinski, BNL Energy Recovery Linac Instrumentation, Proceedings of the 2011 ERL Workshop, WG4-003
13. P. Cameron, et al., "Differential Current Measurements in the BNL ERL Facility", ERL2005 Workshop, Newport News, Virginia, OSTI ID: 15020019. (2010)
14. R. L. Witkover, et al., "RHIC Beam Loss Monitor System Initial Operation", PAC99, p. 2247.

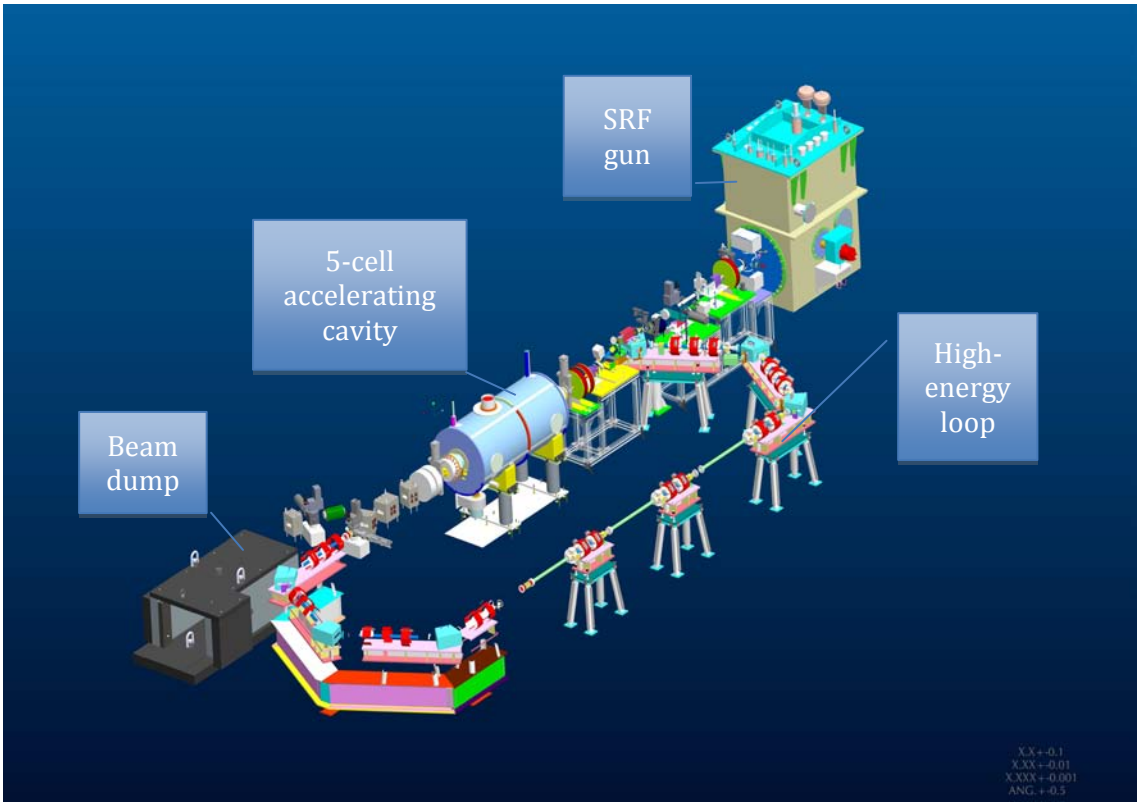

Figure 1. Schematic layout of the R&D Energy Recovery Linac at BNL.